Hindawi
Geofluids
Volume 2021, Article ID 3508806, 11 pages
https://doi.org/10.1155/2021/3508806

Research Article

Study on Prediction of Coal-Gas Compound Dynamic Disaster Based on GRA-PCA-BP Model

Kai Wang,[1,2] Kangnan Li,[1,2] and Feng Du[1,2]

[1]*Beijing Key Laboratory for Precise Mining of Intergrown Energy and Resources, China University of Mining and Technology (Beijing), Beijing 100083, China*
[2]*School of Emergency Management and Safety Engineering, China University of Mining & Technology (Beijing), Beijing 100083, China*

Correspondence should be addressed to Feng Du; fengducumtb@126.com

Received 4 August 2021; Accepted 29 September 2021; Published 14 October 2021

Academic Editor: Qingquan Liu

The intensity and depth of China's coal mining are increasing, and the risk of coal-gas compound dynamic disaster is prominent, which seriously restricts the green, safe, and efficient mining of China's coal resources. How to accurately predict the risk of disasters is an important basis for disaster prevention and control. In this paper, the Pingdingshan No. 8 coal mine is taken as the research object, and the grey relational analysis (GRA), principal component analysis (PCA), and BP neural network are combined to predict the coal-gas compound dynamic disaster. First, the weights of 13 influencing factors are sorted and screened by grey relational analysis. Next, principal component analysis is carried out on the influencing factors with high weight value to extract common factors. Then, the common factor is used as the input parameter of BP neural network to train the previous data. Finally, the coal-gas compound dynamic disaster prediction model based on GRA-PCA-BP neural network is established. After verification, the model can effectively predict the occurrence of coal-gas compound dynamic disaster. The prediction results are consistent with the actual situation of the coal mine with high accuracy and practicality. This work is of great significance to ensure the safe and efficient production of deep mines.

1. Introduction

With the increase of mining intensity and mining depth of China's coal resources, when the coal under high ground stress and high gas pressure is disturbed by mining, the coupling effect of rockburst and coal-gas outburst becomes intense [1–3]. In particular, after entering deep mining, the interaction between rockburst and coal-gas outburst becomes serious, which no longer exists in the form of a single disaster. It shows the characteristics of compound disaster. It is called coal-gas compound dynamic disaster [4–6]. In the process of the occurrence of coal-gas compound dynamic disaster, many factors are intertwined with each other, which may be used as incentives and strengthen each other before, during, and after the accident. Compared with single dynamic disaster, the coupling of two disasters may make the coal-gas compound dynamic disaster more intense and violent, resulting in a large number of property losses and casualties. Coal-gas compound dynamic disaster has become a major disaster restricting the safe and efficient mining of coal resources in China. Therefore, how to accurately predict the occurrence of disasters has become a major scientific issue in the field of coal mine safety under the form of new disasters.

Compared with rockburst and coal-gas outburst, the threshold of coal-gas compound dynamic disaster is lower, and the disaster mechanism is more complex [7–11]. The previous single disaster prediction method is no longer applicable, and the prediction difficulty of coal-gas compound dynamic disaster is greatly increased [12]. At present, the previous research on the prediction of rockburst and coal-gas outburst is quite fruitful [13–18]. However, the research on the prediction of coal-gas compound dynamic disaster is relatively less. Pan [19] put forward three kinds of integrated forecasting technologies, including multi-indexes integrated monitoring of drilling cutting method,

real-time continuous monitoring of coal temperature, and real-time continuous monitoring of coal charge, and applied them in Pingdingshan and other mining areas. Luo et al. [20] used the analytic hierarchy process (AHP) to build a multiparameter risk assessment model of mine dynamic disasters and carried out classification early warning for rockburst, coal-gas outburst, and coal-gas compound dynamic disaster. The model is verified by some examples, and it is concluded that the model has strong applicability to the prediction of dynamic disasters in deep mines. Yuan [21] and Meng and Zhang [22] proposed that through the comprehensive detection method, the coal drilling cutting quantity, the initial gas emission velocity, and the gas desorption quantity should be used as the sensitive indexes for the risk assessment, prediction, and effective inspection of the coal-gas compound dynamic disaster. According to the multifactor coupling unified catastrophe characteristics of deep coal-gas dynamic disaster in Pingdingshan mining area, Yuan [23] proposed the unified prediction theory of deep coal-gas dynamic disaster based on geological dynamic zoning and the probability prediction method of pattern recognition and established the risk evaluation and prediction technical index system of deep coal-gas dynamic disaster in Pingdingshan mining area. By analyzing the correlation between "direction" and "mechanism" of the precursor of coal-gas compound dynamic disaster, Jiang et al. [24] put forward the multiparameter monitoring and joint early warning method of real-time danger. Through the construction of multiparameter joint warning platform, the test is carried out in many coal mines, and the preliminary results are obtained. Dou et al. [25] summarized the monitoring and early warning technologies of gas-earing coal rock dynamic disasters. They include zoning and grading monitoring and early warning, microseism monitoring method, electromagnetic radiation, elastic wave CT and vibration wave CT in the aspect of rock burst monitoring, drilling gas gushing initial velocity method, R-index method, and electromagnetic radiation method in the aspect of coal and gas outburst monitoring. They pointed out that for the monitoring and early warning of coal-gas compound dynamic disaster, we should focus on the establishment of multiparameter normalized dimensionless monitoring and early warning model and criteria for dynamic disaster risk, build the monitoring and early warning index system suitable for coal-gas compound dynamic disaster, and develop the corresponding monitoring technology and equipment.

It can be seen that although relevant scholars have made some meaningful researches on the prediction of coal-gas compound dynamic disaster, most of them are still in the qualitative stage, and the application of quantitative mathematical methods in the prediction of coal-gas compound dynamic disaster is rarely reported. Therefore, combined with the application of mathematical method in the prediction of coal-gas outburst and rockburst [26–29], a method predicting the coal-gas compound dynamic disaster based on the GRA-PCA-BP model is put forward, and the model is verified, and good results are achieved.

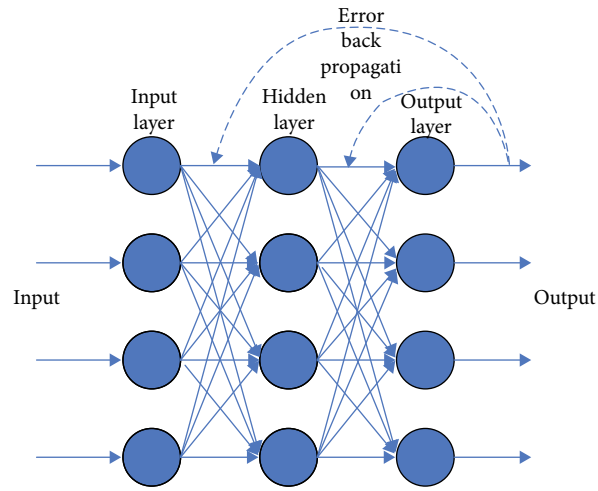

Figure 1: Error back propagation of three-layer network structure.

2. Occurrence Law and Influencing Factors of Coal-Gas Compound Dynamic Disaster

2.1. Occurrence Law of Coal-Gas Compound Dynamic Disaster. Coal-gas compound dynamic disaster is an atypical dynamic disaster induced by mining activities. With the increase of mining depth and complex geological structure, a considerable number of mines are facing the double danger of coal-gas outburst and rockburst. Coal-gas compound dynamic disaster will occur under specific conditions. Based on the field investigation records and extensive literature review of coal-gas compound dynamic disaster in multitime period for multicoal mines, the occurrence laws and destructive characteristics of coal-gas compound dynamic disaster are summarized as follows:

(1) Compared with coal-gas outburst and rockburst, when coal-gas compound dynamic disaster occurs, the critical value of main controlling factors is lower, and the intensity and damage degree of disasters are obviously higher. Compared with the coal-gas outburst disaster, the gas pressure of coal-gas compound dynamic disaster is lower, and the coal strength is higher. Compared with rockburst disaster, when coal-gas compound dynamic disaster occurs, the gas pressure is higher, and the strength of coal seam roof strength is lower

(2) The damage type of coal-gas compound dynamic disaster is obviously different from coal-gas outburst and rockburst, which shows new disaster characteristics. The damage type of coal-gas compound dynamic disaster includes part of the damage characteristics of coal-gas outburst and rockburst disaster. When the coal-gas compound dynamic disaster occurs, the impact power is stronger, and gas emission is higher

2.2. Analysis of Factors Influencing Coal-Gas Compound Dynamic Disaster. To explore the influencing factors of

Table 1: Partial initial data of coal-gas compound dynamic disaster in No. 8 coal mine.

Number	t_1/m	t_2	t_3	t_4	t_5	t_6	t_7	t_8/m	t_9/m	t_{10}/°	t_{11}	t_{12}/mmHg	t_{13}	Disaster or not
1	535	0	0	0	0.5	1.47	3	5.4	0.8	11	0.06	11.23	0.32	1
2	554	0	0.08	0	1	1.47	3	5.4	0.7	11	0.05	15.47	0.28	1
11	566	1	0	0	0.5	1.78	2	3.5	0	16	0	7.93	0.57	1
12	566	1	0	0	0.5	1.78	2	3.5	0	16	0	9.00	0.81	1
20	484	0	0	0	0.5	2.13	3	3.5	0	10	0	12.56	0.29	1
21	530	3	0	0	1	1.72	3	4.3	0.65	24	0.11	11.48	0.67	1
29	540	0	0	0.13	0.5	2.03	3	4.7	1.2	11	0.10	12.05	0.27	1
30	457	0	0	0.14	0.5	1.07	4	3.5	0.4	31	0.06	5.09	0.15	0
38	510	0	0	0	0.5	1.54	3	4.5	1.5	20	0.13	12.74	0.26	1
39	800	1	0.17	0.39	0.5	2.03	3	3.0	0	11	0	15.89	0.18	0

Note: In the column "Disaster or not", the "1" represents that the disaster occurs, and the "0" represents the disaster does not occur.

Table 2: Partial dimensionless data of coal-gas compound dynamic disaster in No. 8 coal mine.

Number	t_1	t_2	t_3	t_4	t_5	t_6	t_7	t_8	t_9	t_{10}	t_{11}	t_{12}	t_{13}	Disaster or not
1	0.9397	0	0	0	0.9331	0.8567	1.0455	1.3431	1.237	0.7863	0.7863	0.8955	0.8746	1
2	0.9731	0	2.7259	0	1.8661	0.8567	1.0455	1.3431	1.0824	0.7863	0.6553	1.2336	0.7653	1
11	0.9942	1.3529	0	0	0.9331	1.0374	0.697	0.8705	0	1.1437	0	0.6323	1.5579	1
12	0.9942	1.3529	0	0	0.9331	1.0374	0.697	0.8705	0	1.1437	0	0.7177	2.2139	1
20	0.8501	0	0	0	0.9331	1.2414	1.0455	0.8705	0	0.7148	0	1.0015	0.7926	1
21	0.9309	4.0588	0	0	1.8661	1.0024	1.0455	1.0695	1.005	1.7156	1.4416	0.9154	1.8313	1
29	0.9485	0	0	1.1178	0.9331	1.1831	1.0455	1.169	1.8555	0.7863	1.31	0.9609	0.738	1
30	0.8027	0	0	1.2037	0.9331	0.6236	1.3939	0.8705	0.6185	2.216	0.7863	0.4059	0.41	0
38	0.8958	0	0	0	0.9331	0.8975	1.0455	1.1192	2.3193	1.4297	1.7037	1.0159	0.7106	1
39	1.4052	1.3529	5.7926	3.3533	0.9331	1.1831	1.0455	0.7461	0	0.7863	0	1.2671	0.492	0

Table 3: Partial correlation coefficient and correlation degree.

Correlation coefficient													
Number	t_1	t_2	t_3	t_4	t_5	t_6	t_7	t_8	t_9	t_{10}	t_{11}	t_{12}	t_{13}
1	0.9046	0.7433	0.7433	0.7433	0.9032	0.8876	0.9272	0.9975	0.9713	0.8737	0.8737	0.8955	0.8912
2	0.9116	0.7433	0.7405	0.7433	0.8842	0.8876	0.9272	0.9975	0.9354	0.8737	0.8489	0.9704	0.8696
11	0.9161	1	0.7433	0.7433	0.9032	0.9255	0.8566	0.8904	0.7433	0.9493	0.7433	0.8447	0.9503
12	0.9161	1	0.7433	0.7433	0.9032	0.9255	0.8566	0.8904	0.7433	0.9493	0.7433	0.8605	0.8199
20	0.8863	0.7433	0.7433	0.7433	0.9032	0.9723	0.9272	0.8904	0.7433	0.86	0.7433	0.9177	0.8749
21	0.9028	0.5915	0.7433	0.7433	0.8842	0.9179	0.9272	0.9325	0.9185	0.9153	0.9779	0.8996	0.8912
29	0.9064	0.7433	0.7433	0.9434	0.9032	0.9585	0.9272	0.9552	0.8863	0.8737	0.9893	0.909	0.8643
30	0.83	1	1	0.765	0.8077	0.8627	0.7376	0.8182	0.8637	0.6388	0.8329	0.9061	0.9053
38	0.8955	0.7433	0.7433	0.7433	0.9032	0.8959	0.9272	0.9437	0.8022	0.9808	0.9178	0.9208	0.8592
39	0.7361	0.7433	0.4035	0.5389	0.8077	0.7681	0.7894	0.84	1	0.8329	1	0.7557	0.8885
Correlation degree													
t_1	t_2	t_3	t_4	t_5	t_6	t_7	t_8	t_9	t_{10}	t_{11}	t_{12}	t_{13}	
0.8804	0.8317	0.7346	0.7556	0.8717	0.8923	0.8712	0.8988	0.8197	0.8717	0.8117	0.8531	0.9077	
Correlation degree ranking													
4	9	13	12	6	3	7	2	10	5	11	8	1	

coal-gas compound dynamic disaster, we need to understand the occurrence and development process of the disaster. Under the influence of mining disturbance, the coal-rock composite structure in critical state begins to deform and lose stability and release elastic strain energy. A large amount of gas expansion energy is accumulated in the pores of coal mass in coal-rock composite structure. The release of gas expansion energy has tensile damage to coal mass. Coal

Table 4: Kaiser-Meyer-Olkin and Bartlett tests.

Kaiser-Meyer-Olkin		0.543
Bartlett sphericity test	Approximate chi-square	91.012
	Degree of freedom	28
	Significance	0

mass failure will further promote the release of elastic energy of coal mass and rock mass. At this time, the overall failure and instability of coal-rock composite structure induce the occurrence of coal-gas compound dynamic disaster. Combined with the influencing factors of coal-gas outburst disaster and rockburst disaster and the occurrence and development process of coal-gas compound dynamic disaster, the preliminary analysis is made to obtain the 13 influence factors of coal-gas compound dynamic disaster, which is buried depth (t_1), fault number (t_2), variation coefficient of coal thickness (t_3), variation coefficient of coal seam dip angle (t_4), soft stratification change (t_5), surrounding rock combination (t_6), type of coal mass failure (t_7), coal thickness (t_8), soft stratification thickness (t_9), coal seam dip angle (t_{10}), wrinkle coefficient (t_{11}), initial velocity of gas emission (t_{12}), and firmness coefficient (t_{13}).

3. Principles of the GRA-PCA-BP Model

3.1. Grey Relational Analysis (GRA). Grey relational analysis is a method of quantitative description and comparison of the development and change situation of a system. By determining the geometric similarity between the reference data column and several comparison data columns, we can judge whether they are closely related, reflecting the degree of correlation between the curves. The grey relational analysis method has several characteristics: it does not need huge data. It can find the corresponding statistical law even in the case of less data. It has no requirement for whether the sample obeys the classical probability distribution function. It will not cause the problem that the qualitative analysis results and quantitative analysis results are inconsistent. The rules and relations of the studied system will not be misinterpreted [30–32].

This method can be used to analyze the correlation degree between each influencing factor and the result when selecting the prediction index of coal-gas compound dynamic disaster. By evaluating the importance of each influencing factor, the main factors affecting the occurrence of coal-gas compound dynamic disaster are screened out from many parameters, and the interference of secondary factors on the prediction process and result is abandoned, which can improve the accuracy of the results and lay a good foundation for the operation of the model.

The specific implementation steps of grey relational analysis are as follows:

(1) Suppose the parent sequence is Y_0, and each influencing factors be the comparison subfactors sequence $Y_i\,(i = 1, 2, \cdots, n)$. The observed values of the parent factors are as follows:

$$Y_0 = \{y_0(1), y_0(2), \cdots, y_0(n)\} \tag{1}$$

The observed values of the subfactors are as follows:

$$Y_{\mathrm{i}} = \{y_i(1), \mathrm{y_i}(2), \cdots, y_i(n)\}. \tag{2}$$

(2) The original data of each sequence are dimensionless processed. Supposing that $X_0, X_i\,(i = 1, 2, \cdots, m)$ are the observed values of parent factor and subfactor, respectively, after dimensionless treatment, then (the average method is used to process the data)

$$x_0(k) = \frac{y_0(k)}{1/n\sum_{t=1}^{n} y_0(t)}, x_i(k) = \frac{y_i(k)}{1/n\sum_{t=1}^{n} y_i(t)} \tag{3}$$

(3) After dimensionless processing of original data, the correlation coefficient ζ between x_0 and $x_i\,(i = 1, 2, 3, \cdots, n)$ at point k is

$$\zeta_i(k) = \frac{\min\limits_i \min\limits_k |x_0(k) - x_i(k)| + \rho \max\limits_i \max\limits_k |x_0(k) - x_i(k)|}{|x_0(k) - x_i(k)| + \rho \max\limits_i \max\limits_k |x_0(k) - x_i(k)|} \tag{4}$$

In formula (4), the formula $\Delta_i(k) = |x_0(k) - x_i(k)|, (i = 1, 2, 3, \cdots, n)$ is called the absolute difference between x_0 and x_i at point k. The formula $\min\limits_i \min\limits_k |x_0(k) - x_i(k)|$ and the formula $\max\limits_i \max\limits_k |x_0(k) - x_i(k)|$ are two-level minimum difference and two-level maximum difference, respectively. The coefficient ρ is the resolution coefficient, generally $\rho = 0.5$.

(4) Calculation of the grey relational degree r_i value

$$r_i = \frac{1}{n}\sum_{k=1}^{n} \zeta_i(k) \tag{5}$$

3.2. Principal Component Analysis (PCA). Principal component analysis (PCA) is a statistical technique to extract common factors from variable groups. This technique can find out the hidden representative factors among many variables and classify the same essential variables into one new factor to effectively reduce the number of variables. This intelligent optimization algorithm has unique advantages in local and global optimization and robust performance.

The advantages of principal component analysis are very suitable for the prediction of coal-gas compound dynamic disaster. The number of factors initially screened by GRA is large, and the correlation between the factors is high. There may be multicollinearity among the factors, which makes the model estimation distorted or difficult to estimate accurately due to the accurate correlation or high correlation

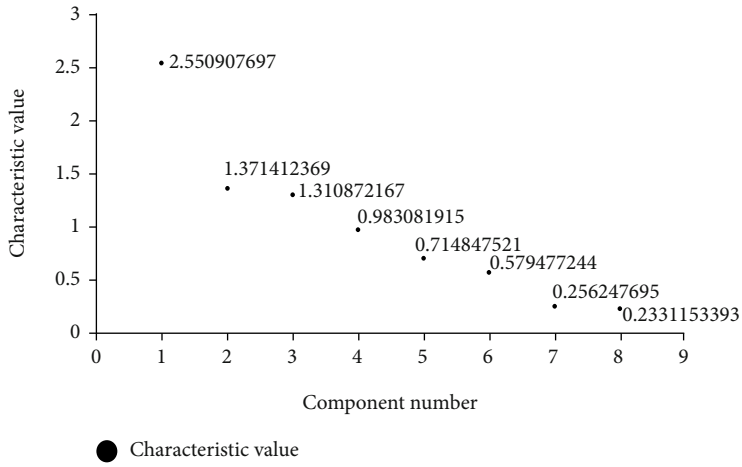

Figure 2: Gravel diagram.

Table 5: Total variance explained.

Total variance explained						
	Initial eigenvalue			Extract the sum of squares of the load		
Common factor	Total	Variance percentage	Cumulative percentage	Total	Variance percentage	Cumulative percentage
1	2.551	31.886	31.886	2.551	31.886	31.886
2	1.371	17.143	49.029	1.371	17.143	49.029
3	1.311	16.386	65.415	1.311	16.386	65.415
4	0.983	12.289	77.703	0.983	12.289	77.703
5	0.715	8.936	86.639			
6	0.579	7.243	93.882			
7	0.256	3.203	97.086			
8	0.233	2.914	100			

Table 6: Composition matrix.

	Component			
	F_1	F_2	F_3	F_4
Buried depth (t_1)	0.576	0.009	-0.661	-0.05
Change of soft stratification (t_9)	0.202	0.286	0.617	0.518
Surrounding rock combination (t_6)	-0.214	0.235	-0.49	0.762
Coal failure type (t_7)	0.844	-0.198	0.145	0.119
Coal thickness (t_8)	0.104	0.717	0.346	-0.19
Coal seam dip angle (t_{10})	-0.098	-0.816	0.328	0.17
Initial velocity of gas emission (t_{12})	0.892	0.082	-0.022	-0.133
Coal firmness coefficient (t_{13})	-0.778	0.095	-0.057	-0.183

between the factors, thus affecting the accuracy of BP neural network prediction. PCA simplification of influencing factors can effectively avoid the occurrence of this problem and can further reduce the dimension of influencing factors by obtaining new common factors [33–35].

The specific implementation steps of principal component analysis are as follows:

(1) Standardized collection of original index data

There are p-dimensional random vector $x = (x_1, x_2, \cdots, x_p)^T$, n samples $x_i = (x_{i1}, x_{i2}, \cdots, x_{ip})^T$, $i = 1, 2, \cdots, n, n > p$, constructing a sample matrix, performing the following standardized transformations on the sample matrix elements:

$$Z_{ij} = \frac{x_{ij} - \bar{x}_j}{s_j}, i = 1, 2, \cdots, n; j = 1, 2, \cdots, p, \quad (6)$$

where $\bar{x}_j = \sum_{i=1}^{n} x_{ij}/n$, $s_j^2 = \sum_{i=1}^{n}(x_{ij} - \bar{x}_j)^2/n - 1$. The normalized matrix Z is obtained.

(2) The correlation coefficient matrix of standardized matrix Z is calculated

$$R = \left[r_{ij}\right]_p xp = \frac{Z^T Z}{n-1}, \quad (7)$$

where $r_{ij} = \sum z_{kj} \cdot z_{kj}/n - 1, i, j = 1, 2, \cdots, p$.

(3) The characteristic equation $|R - \lambda I_p| = 0$ is used to solve the sample correlation matrix R. Then, p characteristic roots are obtained to determine the principal component. Through equation $\sum_{j=1}^{m}\lambda_j / \sum_{j=1}^{p}\lambda_j \geq t$ ($t < 1$), the value of m is determined, which makes the utilization of information more than t. For each $\lambda_j, j = 1, 2, \cdots, m$, the equation $Rb = \lambda_j b$ is solved to get the unit eigenvector b_j^o

(4) The standardized index variables are transformed into main components

$$U_{ij} = z_i^T b_j^o, j = 1, 2, \cdots, m \quad (8)$$

U_1 is the first principal component, U_2 is the second principal component, ..., and U_p is the p principal component.

3.3. BP Neural Network. BP neural network is a kind of multilayer feedforward neural network trained according to the error back propagation algorithm, which is the most widely used neural network [36, 37]. The topological structure of BP neural network model is composed of three layers: input layer, hidden layer, and output layer. Gradient shrinkage technique is used to calculate the solution weight by iterative operation. The addition of hidden nodes makes the adjustable parameters increase and approach the accurate value. There is no uniform regulation on the number of neurons in the implied layer, which is generally determined by empirical formula. The empirical formula for determining the number of neurons N in the hidden layer is as follows:

$$N = \sqrt{n \times m}, \quad (9)$$

$$N = \sqrt{n \times m} + a, \quad (10)$$

$$N = \mathrm{m}(n + 1), \quad (11)$$

$$N = 2m + 1, \quad (12)$$

where n is the number of input layer nodes, m is the number of output layer nodes, and a is a constant between 1 and 10. From the input layer to the hidden layer and from the hidden layer to the output layer, the actual output value is obtained. When the output layer error exceeds the error tolerance range, it will be back propagation. By modifying the weights of the neural nodes, the mean square error of the expected output and the actual output is minimized. Therefore, the results meet the requirements. The structure diagram is shown in Figure 1.

Table 7: Some common factor data after calculation.

Number	X_1	X_2	X_3	X_4
1	1.60969737	0.74749536	0.339417928	0.812900035
2	2.204036798	1.03198924	0.891851959	1.269598519
11	0.457772706	0.272297774	0.084938237	0.966876527
12	0.02353326	0.341611389	0.045670799	0.835486048
20	1.592037485	0.557492709	0.025542212	1.189012618
21	0.915941684	0.186560304	1.004711086	1.439935842
29	1.691453877	0.691818614	0.119806084	1.110542908
30	1.610308877	-0.967254621	0.937421456	1.166563328
38	1.724334178	0.065505757	0.48872312	1.012079589
39	2.375037821	0.394508286	-0.321069244	1.172335713

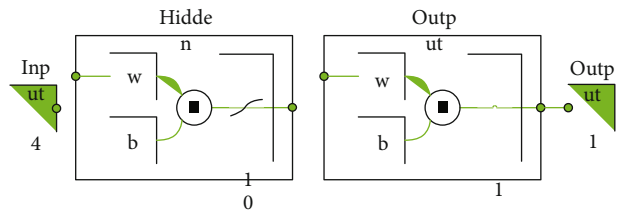

Figure 3: BP neural network model.

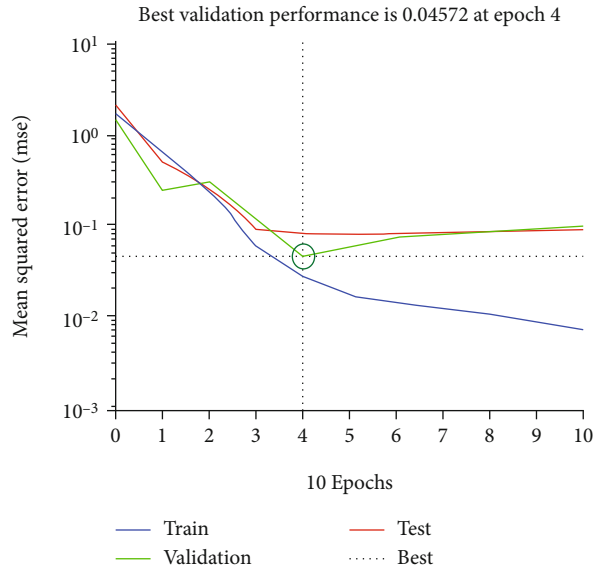

Figure 4: Working performance of neural network.

3.4. GRA-PCA-BP Model. In the GRA-PCA-BP model, firstly, the influencing factors with high weight are screened by grey relational analysis. Secondly, the influencing factors

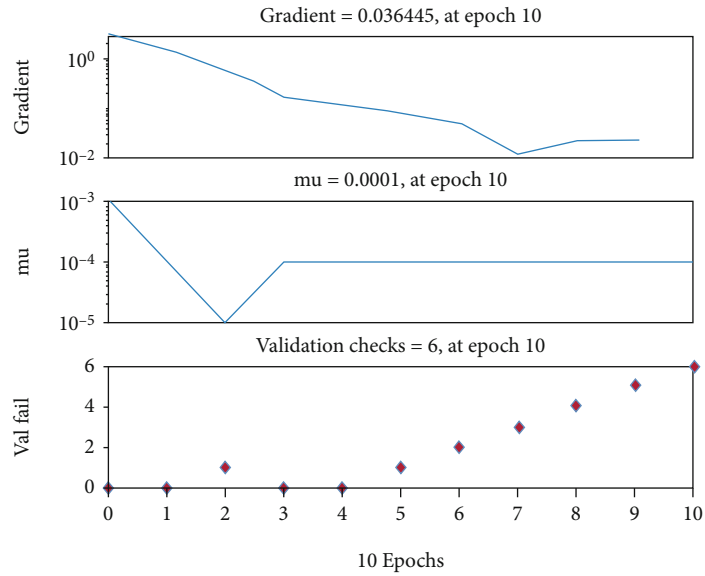

Figure 5: Training status diagram.

are integrated into representative common factors through principal component analysis, and the number of factors is further reduced. Finally, the common factor data is substituted into the input layer of BP neural network, and the training of prediction model is started to obtain a model that can accurately predict whether disasters occur. Grey relational analysis eliminates irrelevant or small influence factors. Principal component analysis eliminates multicollinearity between independent variables and further reduces the dimension of input data. The BP neural network has good predictability. The combination of the three methods can make full use of the advantages and avoid the disadvantages and can accurately and quickly predict the coal-gas compound dynamic disaster.

4. Case Analysis

4.1. Grey Relational Analysis of Influencing Factors. The influencing factors of 13 kinds of coal-gas compound dynamic disasters were analyzed. In this paper, we need to compare the 13 factors with whether the occurrence of compound disasters and calculate the correlation degree, so the parent sequence Y_0 is whether the occurrence of compound disasters. The 46 groups of data of Pingdingshan No. 8 coal mine are selected and analyzed by the SPSS software. Some initial data are shown in Table 1, some dimensionless data are shown in Table 2, and correlation coefficient and correlation degree are shown in Table 3.

Through the process of grey relational analysis, the order of 13 factors affecting the strength of coal-gas compound dynamic disaster is obtained: coal firmness coefficient (t_{13}) >coal thickness (t_8)>surrounding rock combination (t_6) >buried depth (t_1)>coal seam dip angle (t_{10})>change of soft stratification (t_5)>coal failure type (t_7)>initial velocity of gas emission (t_{12})>number of faults (t_2)>thickness of soft stratification (t_9)>wrinkle coefficient (t_{11})>variation coefficient of coal seam dip angle (t_4)>variation coefficient of coal thickness (t_3). Some of the influencing factors with a small degree of relevance (less than 0.85) are deduced, and the first eight influencing factors are kept.

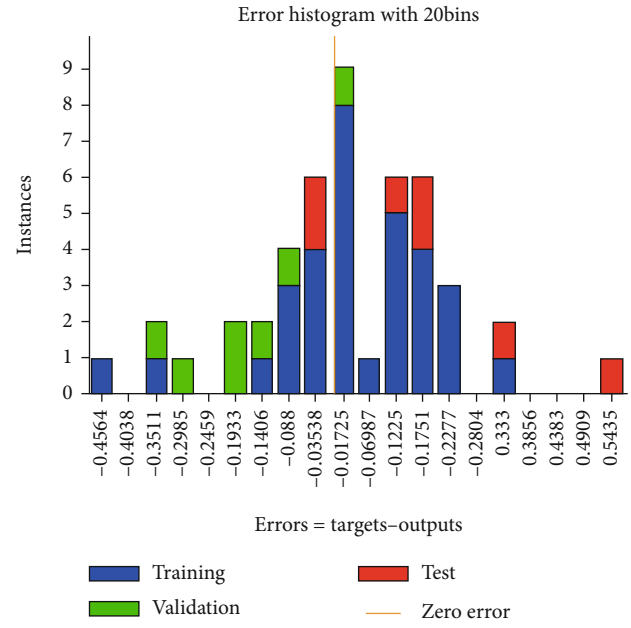

Figure 6: Error histogram.

4.2. Using PCA to Simplify the Main Influencing Factors. The first eight retained factors were simplified by PCA using the SPSS software. After the process of inspection, extraction, and calculation, four common factor data were finally obtained. The following are the specific steps.

KMO (Kaiser-Meyer-Olkin) and Bartlett test results are shown in Table 4. KMO test statistics show whether the partial correlation between variables is strong enough. Bartlett sphericity test is used to judge whether the correlation

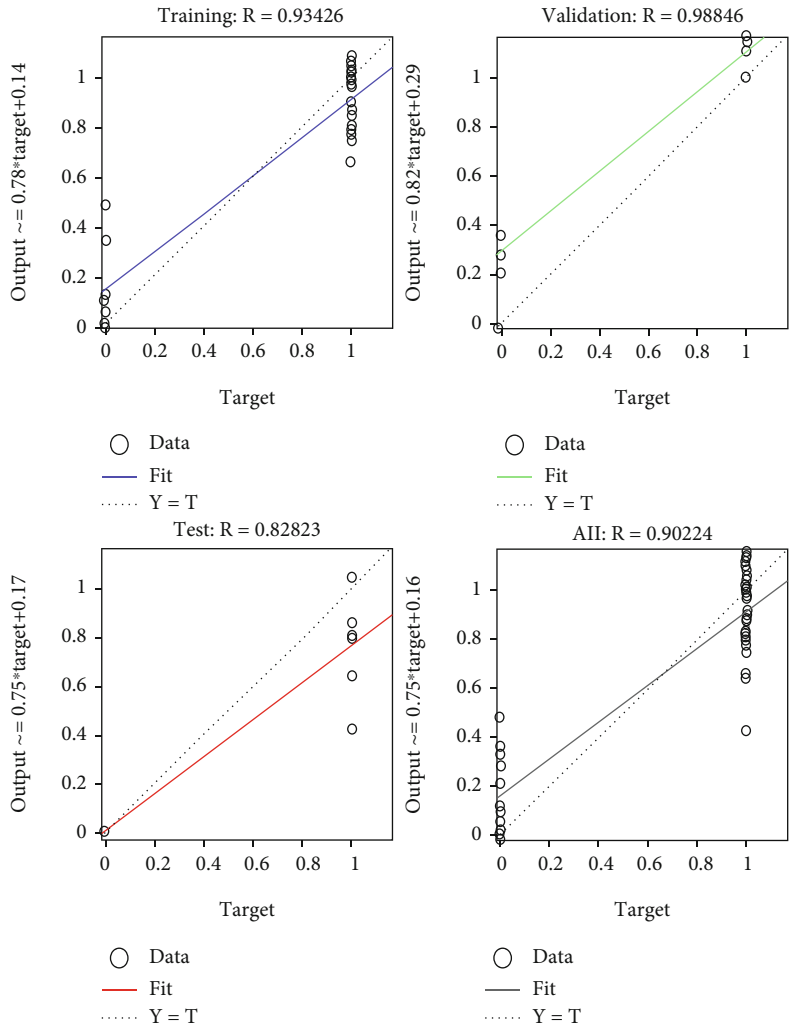

Figure 7: Linear regression analysis.

matrix is the identity matrix. It can be seen from Table 4 that the value of KMO test statistic is 0.543, which indicates that the degree of information overlap among the variables is acceptable and can be used for principal component analysis. In Bartlett's sphericity test, the value of significance is 0, which indicates that the hypothesis that each variable is independent is rejected and there is a strong correlation between variables.

Figure 2 is the gravel diagram, and Table 5 shows the explanation of total variance. The horizontal axis of the gravel diagram is the number of each common factor, and the vertical axis represents the size of its characteristic value. The diagram can intuitively get the importance of each common factor. The detailed information of each common factor is listed on the left side of the total variance explanation table, and the information of extracting the common factor is on the right side. It can be seen from Figure 2 and Table 5 that the eigenvalues of the first four common factors are close to or greater than 1, and the sum of the variance percentages reaches 77.7%, that is, the first four common factors can represent eight influencing factors.

Table 6 is the component matrix, and Table 7 shows part of the calculated common factor data. Component matrix, also known as factor load matrix, is the coefficient of the factor expression of each original variable, which expresses the influence degree of the extracted common factor on the original variable. Through the factor load matrix, we can get the linear combination of the original index variables, such as $X_1 = a_{11} \times F_1 + a_{12} \times F_1 + a_{13} \times F_1 + \cdots + a_{18} \times F_1$, where X_1 is the common factor data 1. a_{11}、a_{12}、$a_{13} \cdots a_{18}$ are the factor loads on the same line as component F_1. F_1 is the extracted component.

4.3. Construction of BP Neural Network. As shown in Figure 3, this paper uses the MATLAB software to build a neural network model, repeatedly trains and verifies the common factor data, and finally obtains a model that can effectively predict coal-gas compound dynamic disaster.

The MATLAB software includes input layer, hidden layer, and output layer. The common factor data in Table 7 takes the output type of numerical matrix as the input data of BP neural network, and the output type of

Table 8: Prediction results of common factor test set of coal-gas compound dynamic disaster.

Number	X_1	X_2	X_3	X_4	Forecast results	Expected results
44	1.399042495	0.785939655	-0.11810208	1.141111803	1	1
45	1.190427325	0.760470516	-0.219058963	1.091743892	1	1
46	2.44822473	-0.227521877	0.287181263	1.03121518	0	0

numerical matrix is taken as the output data of BP neural network in the column of "Disaster or not" in Table 1.

The 32 sets (70%) of data are randomly selected as the training set. The 7 sets (15%) of data are selected as the validation set. The other 7 sets (15%) of data are selected as the test set. For the number of neurons in the hidden layer, formula (9) is used for calculation, $a = 8$. Thus, the prediction model structure is set as a 3-layer 4-10-1 structure.

During the model training, the parameters are set as follows: the maximum number of network training is set to 1000 times, the training accuracy is set to 0.0001, and the learning rate is set to 0.01.

Figure 4 shows the performance of the neural network. The ordinate is the mean square error, and the abscissa is the number of iterations. It can be seen from the figure that after training the neural network using the Levenberg-Marquardt method, the number of iterations of the neural network is very small, and the network training is completed in only 10 steps. And the best verification of the neural network is obtained when the number of iteration steps is 4. The square error value is 0.04572.

Figure 5 shows the visualization of gradient, Mu factor, and generalization ability transformation in the network training process. It can be seen from the figure that the actual gradient of the network is 0.036, and the actual value of the damping factor Mu in the Levenberg-Marquardt algorithm used by the network is $1e^{-4}$. Validation checks indicate the generalization ability check standard of the network. If the training error cannot be reduced for 6 consecutive times, the training task will be ended.

Figure 6 shows the error histogram. In the figure, the abscissa represents the median of the error interval, and the ordinate represents the number of samples located in the error interval. From this figure, the error between the output value of the neural network and the original target value of the sample can be obtained.

Figure 7 shows the fitting results of the linear regression analysis of the test set, training set, and validation set. From the figure, the regression fitting situation of the data can be obtained. The regression R value measures the correlation between the output and the target. An R value of 1 indicates a close relationship, and 0 indicates a random relationship. The overall R value of the three sets is 0.90224, indicating that the regression fitting effect is good.

4.4. Test of GRA-PCA-BP Model. The last three groups of data are selected to input the model for prediction, testing whether the model constructed in this paper meets the target requirements. The prediction results are shown in Table 8. From the prediction results, it can be seen that the prediction results of GRA-PCA-BP model are completely consistent with the actual situation, which indicates that this method is feasible to predict the risk of coal-gas compound dynamic disaster and has good promotion value in practice.

5. Conclusion

The prediction of coal-gas compound dynamic disaster is of great significance for the safe and efficient mining of coal mine. Firstly, the grey relational analysis method is used to eliminate irrelevant or small influential factors, and then, the principal component analysis method is used to eliminate the multicollinearity between the independent variables. Moreover, the input data dimension is further reduced. Combined with the good prediction effect of BP neural network, the coal-gas compound dynamic disaster prediction model based on GRA-PCA-BP is finally obtained. The model has high prediction accuracy and convenient operation.

Model verification of the disaster case of Pingdingshan No. 8 mine shows that the coal-gas compound dynamic disaster prediction model based on GRA-PCA-BP neural network has high accuracy and practicability, which provides a new method for the disaster prediction of the coal mines with coal-gas compound dynamic disaster risk, and provides a theoretical basis for the safe and efficient mining of coal resources in deep mining areas in China.

To the best of our knowledge, this is the first work using mathematical methods to predict coal-gas compound dynamic disaster. But only relying on the limited data of Pingdingshan No. 8 mine for research, the accuracy still needs to be verified by using more data of the coal mine. Meanwhile, the model used in this article is relatively simple. It is necessary to continue to study more accurate mathematical models to accurately predict coal-gas compound dynamic disaster. This is our focus in the future.

Data Availability

The data used to support the findings of this study are available from the corresponding author upon request.

Additional Points

Bullet Points. (1) The influencing factors of coal-gas compound dynamic disaster were analyzed. (2) A prediction model of coal-gas compound dynamic disaster based on GRA-PCA-BP was established. (3) The prediction model is verified by the case study of Pingdingshan No. 8 coal mine.

Conflicts of Interest

All the authors declare that they have no conflict of interest.

Authors' Contributions

Kai Wang contributed to the formal analysis and writing—original draft. Kangnan Li contributed to the investigation and writing—review and editing. Feng Du contributed to the methodology, investigation, writing—review and editing, and supervision.

Acknowledgments

This research was funded by the National Natural Science Foundation of China (52130409, 52121003, 51874314, and 52004291).

References

[1] Q. Tu, Y. Cheng, Q. Liu et al., "Investigation of the formation mechanism of coal spallation through the cross-coupling relations of multiple physical processes," *International Journal of Rock Mechanics & Mining Sciences*, vol. 105, pp. 133–144, 2018.

[2] K. Wang, A. Zhou, J. Zhang, and P. Zhang, "Real-time numerical simulations and experimental research for the propagation characteristics of shock waves and gas flow during coal and gas outburst," *Safety Science*, vol. 50, no. 4, pp. 835–841, 2012.

[3] H. Xie, Y. Ju, F. Gao, M. Gao, and R. Zhang, "Groundbreaking theoretical and technical conceptualization of fluidized mining of deep underground solid mineral resources," *Tunnelling & Underground Space Technology*, vol. 67, pp. 68–70, 2017.

[4] K. Wang and F. Du, "Coal-gas compound dynamic disasters in China: a review," *Process Safety and Environmental Protection*, vol. 133, pp. 1–17, 2020.

[5] C. P. Lu, L. M. Dou, N. Zhang, J. H. Xue, and G. J. Liu, "Microseismic and acoustic emission effect on gas outburst hazard triggered by shock wave: a case study," *Natural Hazards*, vol. 73, no. 3, pp. 1715–1731, 2014.

[6] F. Du and K. Wang, "Unstable failure of gas-bearing coal-rock combination bodies: insights from physical experiments and numerical simulations," *Process Safety and Environmental Protection*, vol. 129, pp. 264–279, 2019.

[7] P. Konicek, K. Soucek, L. Stas, and R. Singh, "Long-hole destress blasting for rock-burst control during deep underground coal mining," *International Journal of Rock Mechanics and Mining Sciences*, vol. 61, pp. 141–153, 2013.

[8] Q. T. Hu, S. T. Zhang, G. C. Wen, L. Dai, and B. Wang, "Coal-like material for coal and gas outburst simulation tests," *International Journal of Rock Mechanics and Mining Sciences*, vol. 74, pp. 151–156, 2015.

[9] T. Li, M. F. Cai, and M. Cai, "A review of mining-induced seismicity in China," *International Journal of Rock Mechanics and Mining Sciences*, vol. 44, no. 8, pp. 1149–1171, 2007.

[10] F. Du, K. Wang, X. Zhang, C. Xin, L. Shu, and G. Wang, "Experimental study of coal-gas outburst: insights from coal-rock structure, gas pressure and adsorptivity," *Natural Resources Research*, vol. 29, no. 4, pp. 2481–2493, 2020.

[11] X. L. Li, S. J. Chen, Z. H. Li, and E. Y. Wang, "Rockburst mechanism in coal rock with structural surface and the microseismic (MS) and electromagnetic radiation (EMR) response," *Engineering Failure Analysis*, vol. 124, no. 6, p. 105396, 2021.

[12] B. Gao, F. Mi, and R. Zhang, "Research status and prospect of compound dynamic disaster of deep mining in coal mine," *Coal mine safety*, vol. 44, no. 11, pp. 175–178, 2013.

[13] C. WANG, E. WANG, X. U. Jiankun, X. LIU, and L. LING, "Bayesian discriminant analysis for prediction of coal and gas outbursts and application," *Mining Science and Technology (China)*, vol. 20, no. 4, pp. 520–523, 2010.

[14] B. Jta, D. Cwc, B. Yca et al., "Determination of critical value of an outburst risk prediction index of working face in a coal roadway based on initial gas emission from a borehole and its application: a case study," *Fuel*, vol. 267, p. 117229, 2020.

[15] J. Tang, C. Jiang, Y. Chen, X. Li, G. Wang, and D. Yang, "Line prediction technology for forecasting coal and gas outbursts during coal roadway tunneling," *Journal of Natural Gas Science & Engineering*, vol. 34, pp. 412–418, 2016.

[16] L. Qiu, Z. Liu, E. Wang, X. He, J. Feng, and B. Li, "Early-warning of rock burst in coal mine by low-frequency electromagnetic radiation," *Engineering Geology*, vol. 279, no. 1, p. 105755, 2020.

[17] C. Zhang, G. Jin, C. Liu et al., "Prediction of rockbursts in a typical island working face of a coal mine through microseismic monitoring technology," *Tunnelling and Underground Space Technology*, vol. 113, p. 103972, 2021.

[18] X. Li, F. Pan, H. Li, M. Zhao, L. Ding, and W. Zhang, "Prediction of rock-burst-threatened areas in an island coal face and its prevention: a case study," *International Journal of Mining Science and Technology*, vol. 26, no. 6, pp. 1125–1133, 2016.

[19] Y. Pan, "Integrated study on compound dynamic disaster of coal-gas outburst and rockburst," *Journal of coal industry*, vol. 41, no. 1, pp. 105–112, 2016.

[20] Y. Luo, Y. Pan, and X. Xiao, "Multi-parameter risk evaluation and graded early warning of mine dynamic disaster," *Chinese Journal of Safety Science*, vol. 23, no. 11, pp. 85–90, 2013.

[21] R. Yuan, "Features of dynamic disasters combined rockburst and gas outburst in deep coal mine and its preventive measures," *Coal science and technology*, vol. 41, no. 8, pp. 6–10, 2013.

[22] X. Meng and Y. Zhang, "Temporal evolution of stress field-based drilling method outburst prediction theory and practice. Intelligent Information Technology Application Association," in *Proceedings of 2011 AASRI conference on information technology and economic development (AASRI-ITED 2011 V1). Intelligent Information Technology Application Association: Intelligent information technology application society*, p. 4, Kuala Lumpur, Malaysia, 2011.

[23] R. Yuan, *Study on the Disaster Mechanism and Prevention Key Technologies of Deep Mine Dynamic Disasters in Pingdingshan Coal Mine*, China University of mining and Technology, 2012.

[24] F. Jiang, G. Yang, and Q. Wei, "Study and prospect on coal mine composite dynamic disaster real-time prewarning platform," *Journal of coal industry*, vol. 43, no. 2, pp. 333–339, 2018.

[25] L. Dou, X. He, and R. E. N. Ting, "Mechanism of coal-gas dynamic disasters caused by the superposition of static and dynamic loads and its control technology," *Journal of China University of Mining and Technology*, vol. 47, no. 1, pp. 48–59, 2018.

[26] S. Jian, W. Lian-guo, Z. Hua-lei, and S. Yi-feng, "Application of fuzzy neural network in predicting the risk of rock burst,"

Procedia Earth and Planetary Science, vol. 1, no. 1, pp. 536–543, 2009.

[27] Y. Li, Y. Yang, and B. Jiang, "Prediction of coal and gas outbursts by a novel model based on multisource information fusion," *Energy Exploration & Exploitation*, vol. 38, no. 5, article 014459872091307, pp. 1320–1348, 2020.

[28] S. Wu, Z. Wu, and C. Zhang, "Rock burst prediction probability model based on case analysis," *Tunnelling and underground space technology*, vol. 93, p. 103069, 2019.

[29] B. Li, E. Wang, Z. Shang et al., "Deep learning approach to coal and gas outburst recognition employing modified AE and EMR signal from empirical mode decomposition and time-frequency analysis," *Journal of Natural Gas Science and Engineering*, vol. 90, p. 103942, 2021.

[30] S. J. Ren, C. P. Wang, Y. Xiao et al., "Thermal properties of coal during low temperature oxidation using a grey correlation method," *Fuel*, vol. 260, p. 116287, 2020.

[31] Q. Nian, S. Shi, and R. Li, "Research and application of safety assessment method of gas explosion accident in coal mine based on GRA-ANP-FCE," *Procedia Engineering*, vol. 45, no. 2, pp. 106–111, 2012.

[32] X. Yang and W. Li, "Research on coal mine safety accident based on grey relational analysis," *Innovative Computing and Information*, vol. 231, pp. 101–108, 2011.

[33] X. Yang and Z. Su, "Prediction of the protein O-glycosylation by kernel principal component analysis and support vector machines," *Science technology and Engineering*, vol. 13, no. 25, pp. 7371–7376, 2013.

[34] T. Parhizkar, E. Rafieipour, and A. Parhizkar, "Evaluation and improvement of energy consumption prediction models using principal component analysis based feature reduction," *Journal of Cleaner Production*, vol. 279, p. 123866, 2021.

[35] A. Roy, H. Dhawan, S. Upadhyayula, and H. Kodamana, "Insights from principal component analysis applied to Py-GCMS study of Indian coals and their solvent extracted clean coal products," *International Journal of Coal Science & Technology*, 2021.

[36] Y. Wu, R. Gao, and J. Yang, "Prediction of coal and gas outburst: a method based on the BP neural network optimized by GASA," *Process Safety and Environmental Protection*, vol. 133, pp. 64–72, 2020.

[37] C. Y. Ping, "An incorporate genetic algorithm based back propagation neural network model for coal and gas outburst intensity prediction," *Procedia Earth and Planetary Science*, vol. 1, no. 1, pp. 1285–1292, 2009.